Eur Radiol (2006) 16: 2427–2443
DOI 10.1007/s00330-006-0247-9

J. T. Winterer
E. Kotter
N. Ghanem
M. Langer

Detection and characterization of benign focal liver lesions with multislice CT

Received: 12 July 2005
Revised: 17 February 2006
Accepted: 2 March 2006
Published online: 25 May 2006

J. T. Winterer (✉) · E. Kotter · N. Ghanem · M. Langer
Department of Diagnostic Radiology,
Hugstetter Str. 55,
D-79106 Freiburg, Germany
e-mail: jan.winterer@klinikum.uni-freiburg.de
Tel.: +49-761-2703802
Fax: +49-761-2703956

Abstract MDCT is a rapidly evolving technique that significantly improves CT imaging for several indications including depiction of focal benign lesions. Imaging mainly profits from improved longitudinal spatial resolution allowing high-quality non-axial reformations and 3D reconstructions and CT angiography as well as rapid accurate multiphase imaging with short breath-holding periods. This review provides an overview of the current status of MDCT with respect to liver imaging and the implications for characterizing benign focal liver lesions. MDCT currently allows the acquisition of thin slices in daily routine diagnostics providing an improved detection rate of small liver lesions. Whereas large benign focal liver lesions exhibit typical patterns of morphology, attenuation and perfusion, which also may be assessed with single-slice scanners, small lesions remain challenging even with MDCT, since the specific criteria for confident diagnosis become more ambiguous. Here, MR imaging provides more detailed information about tissue components and the availability of liver-specific contrast agents, adding further impact to this technique. With respect to dose considerations, the number of necessary multiphase scans as well as the application of very thin collimation should be strictly checked for each patient undergoing MDCT based on the individual clinical situation and question.

Keywords Liver neoplasms · Diagnostic imaging · Multidetector CT · Spiral computed tomography

Introduction

The advent of the multirow detector technique has lead to a renaissance of CT in recent years, and with the exception of soft tissue and joint diagnostics, CT is now used as a basic approach to the whole body as radiography was in earlier years. Besides thoracic and vessel diagnostics, the assessment of the abdomen is the main role for CT examination, where the major indication is to detect or exclude and characterize focal liver lesions (1) in patients where a primary malignancy is already known in order to search for metastasis and (2) in individuals with a suspected tumor in order to discover the primary site of the malignancy.

Although MRI has gained a increasing role in liver imaging, the availability and widespread distribution makes CT still the most commonly used method for upper abdomen diagnostics [1].

Imaging diagnostics of the liver are hampered by the fact that 20–50% of the population exhibit benign focal lesions, mostly cysts and hemangioma, lowering the pretest probability of identifying malignant instances [2]. In addition, MRI, CT, and ultrasound (US) provide increasing spatial resolution, improving the likelihood of disclosing very small changes with uncertain dignity.

Multidetector CT (MDCT) was introduced into diagnostic imaging in 1998. The initial breakthrough was followed by extensive technical efforts to improve the multislice technology by increasing the number of rows within the detector unit. Due to intense worldwide efforts of commercial developers, the time cycles for scanner

innovations have grown shorter and shorter. Whereas in 2001, 16-slice systems again revolutionized CT imaging, just 3 years later 64-slice scanners were available.

The advantage of MDCT is that multiple images during a single rotation are obtained simultaneously, multiplying the amount of digital image data by the number of detector rows. This feature basically can be translated into two advances: (1) established spatial resolution but increased z-axis coverage speed supported by subsecond rotation speed implemented in the latest scanner systems, or (2) improved longitudinal resolution providing an almost isotropic data set.

Faster scanning allows for anatomic coverage of large fields of view as might be necessary in trauma management or for ultrashort examination times which may lower motion artifacts in dyspnoic patients. Faster scanning also allows acquisition of high-resolution multiphase data sets with sharper distinction of each perfusion phase. Maximizing longitudinal resolution is particularly apt for excellent 3D reconstructions commonly being requested by referring physicians for preoperative visualization of vessel anatomy or clarification of interfaces that are predominantly situated in the z-axis.

Liver depiction may profit from both faster z-axis scanning translated into improved perfusion imaging and from higher longitudinal resolution translated into reduced partial volume effects, which may occur in the dome of the liver or at the liver margins. Furthermore, nearly isotropic data sets allow smooth and detailed multiplanar reformation with clear distinction of the liver margins from the surrounding tissue allowing for more confident assessment of whether there is extrahepatic growth of a tumor or not. In addition, better through-plane resolution makes high-quality two- or three-dimensional reconstruction of the arterial and portal venous vessel tree possible. These data help to clarify vascular involvement in pathologic changes and furthermore provide a roadmap for possible surgical interventions.

With respect to clinical demands, the capabilities of MDCT have to be focused on concrete indications for the liver scan. For diagnosing a focal benign or malign lesion the role of CT is to demonstrate the nature of the tumor and its relationship to the surrounding liver tissue and vessels as well as the extrahepatic structures. In this regard CT has to be highly reliable and specific in order to avoid further investigations and to give the best image to the referring physicians for possible intervention. In cases of extrahepatic disease, the role of CT is to rule out intrahepatic metastasis where maximum sensitivity and negative predictive value are requested.

The key imaging features of benign liver lesions such as hemangioma or FNH are well known from several studies undertaken with single-slice CT (SSCT) in recent years [3–5]. To what extent the theoretical advantages of MDCT translate into significant diagnostic improvement compared to single-slice CT for assessing focal liver lesions is still a matter in question.

The same applies to whether liver CT derives any benefit from the evolution to 64-detector-row scanners from 16-row. Indeed, even with 4-row scanners, thin-slice multiphase data sets with short breath-holding periods are possible. However, overbeaming was a substantial problem in the early MDCT systems with up to 4 detector rows since relevant radiation exposure occurs at the margins of the beam fan, which can not be translated into image reconstruction but contributes to an increase of the patient's effective dose. This drawback is almost negligible in the advanced scanners with at least 16 rows [6]. However, until now, there has been no concrete evidence as to whether increasing the number of detector rows beyond 16 is of any further benefit for liver CT with respect to detection and characterization of focal tissue lesions.

Technical aspects of MDCT

In 1998, all major CT manufacturers introduced the 4-slice CT systems that now are the minimum standard for MDCT. Following that, the race to increase the number of simultaneously acquired detector rows started. The introduction of 16-detector-row scanners with subsecond gantry rotation substantially improved z-axis resolution and decreased the necessary time for longitudinal scanning.

Table 1 Technical parameters for evolution within one scanner family featuring increasing number of detector sections (Siemens Medical Solutions, Erlangen, Germany)

	Single section, Siemens Emotion	4 section, Siemens Volume Zoom	16 section, Siemens Sensation 16	64 section, Siemens Sensation 64
Collimation	1×5	4×2.5	16×1.5	20×1.2
Table feed	8 mm	15 mm	24 mm	24 mm
Pitch	1.5	1.5	1.0	1.0
Slice thickness	5 mm	5 mm	5 mm	5 mm
Rotation time	1.0 s	0.5s	0.5 s	0.5 s
Scan time[a]	30 s	8 s	5 s	5 s

[a]Scan length=24 cm

Currently, 64-row systems are established in clinical routine and provide true isotropic image voxels with a minimum 0.4 mm size and 0.37 s gantry rotation time. Table 1 demonstrates the evolution of the relevant technical parameters within the scanner family of one manufacturer (Siemens Medical Solutions, Erlangen, Germany). Table 2 shows an overview of the technical advances with increasing numbers of detector rows for several vendors.

In simple terms, compared to single-slice CT, the spatial information obtained during one X-ray tube rotation is multiplied by the number of detector rows being implemented in the MDCT system. However, increasing the number of detector rows implies a variety of non-trivial physical problems that had to be resolved to avoid heavy reconstruction artifacts. The available 4-row scanners neglect the cone angle of the measurement rays. While this is justified for 4 slices, it creates severe artifacts such as heavy streaks and geometrical distortions if applied to 16 or more slices [7]. To resolve these artifacts sophisticated z-reformation algorithms such as the Adaptive Multiple Plane Reconstruction (AMPR) have been developed [7].

MDCT devices, more than single-slice CT devices, are substantially manufacturer-dependent with respect to the tube-detector array unit, data acquisition including the management of tube current, gantry rotation, adapted table feed, and the reconstruction of the digital data readout. In order to provide a maximum spectrum of imaging settings for z-axis resolution, pitch, increment, and dose demand, the concept of the adaptive detector array is the preferred approach of data acquisition particularly in scanners with more than 4 detector rows [11]. The possible spatial resolution of the latest 64-detector-row systems even exceeds the proposed setting for liver imaging since dose-reducing considerations in routine examinations require more and more attention (Tables 2, 3). As shown in Table 3, the beam collimation and detector readout are set below the potential in the 16-row and 64-row systems due to dose considerations.

Table 2 Collimation presettings for MDCT scanners of several manufacturers with increasing numbers of detector rows

	4 slice	16 slice	64 slice
Siemens	2×0.5 mm	16×0.75 mm	32×0.6 mm
	4×1.0 mm	16×1.50 mm	
	4×2.5 mm		
	4×5.0 mm		64×0.4 mm[a]
	2×10 mm		
Philips	2×0.5 mm	16×0.75 mm	64×0.625 mm
	4×1.0 mm	16×1.50 mm	
	4×2.5 mm		
	4×5.0 mm		
	2×10 mm		
General Electric	2×0.63 mm	16×0.625 mm	64×0.625 mm
	4×1.25 mm	16×1.250 mm	
	4×2.50 mm		
	4×3.75 mm		
	4×5.0 mm		
	2×10.0 mm		
Toshiba	4×0.5 mm	16×0.5 mm	64×0.5 mm
	4×1.0 mm	16×1.0 mm	
	4×2.0 mm	16×2.0 mm	
	4×3.0 mm		
	4×5.0 mm		
	4×8.0 mm		

[a]STRATON tube with double "flying" z-spot data readout

The manufacturers commonly provide a user-friendly spectrum of organ protocols with the relevant technical parameters preset in order to ensure optimum image quality with respect to signal-to-noise ratio, dose application and spatial resolution. MDCT protocols for multiphase liver imaging profit from the given thin detector collimations since volume data sets can be reconstructed for the particular clinical question and indication. Using a 16-slice scanner, the arterial dominant phase scanning can be reconstructed with slice width/increment 5 mm/5 mm for diagnostic purposes, and in a second step, with slice width/increment 1 mm/0.7 mm for CT angiography as well as perfect and near isotropic multiplanar reformations (see Table 3).

Collimation of 0.75–2.5 mm and pitch of 1–1.5 are advisable depending on the scanner type and particularly on the number of detector rows. With MDCT, a typical cranio-caudal span for liver imaging of 20–30 cm can be scanned in less than 10 s allowing for short breath-holding and optional accurate triple-phase acquisition, including an early arterial phase at an injection delay of approximately 20 s. The effective dose for liver depiction is ultimately determined by the user's demands in terms of image quality as a tradeoff between collimation, pitch and signal-to-noise. Common values are 140–160 mAs but may have to be adapted individually to the patient's constitution, particularly the patient's weight. Table 3 shows a protocol for triple-phase liver MDCT with use of automated bolus triggering and acquisition of a precontrast scan.

The great technical performance of MDCT tempts one to use this technique more extensively in daily routine diagnostics than may be necessary for diagnostic purposes. This concerns the acquisition of thinner slices as well as an increased number of multiphase series for obtaining more detailed perfusion data when using a contrasting agent. Indeed, a national survey in Germany demonstrated that the introduction of MDCT initially led to a markedly increased number of examinations [8]. Although very thin slices can be obtained during breath-holding periods, the early MDCT scanners with up to 4 detector rows, in particular, exhibit a poor dose efficiency due to severe overbeaming in case of high-resolution acquisition [9]. This issue has become less significant in the latest systems with 16 and

Table 3 Scan protocol for triple-phase liver study with a 16-section MDCT scanner (Siemens Somatom Sensation 16)

	Native	Timing bolus[a]	Early arterial	Late arterial	Hepatic vein
kV	120	120	120	120	120
Effective mAs	140	20	160	140	140
Slice collimation	1.5 mm	16×1.5 mm	16×0.75 mm	16×1.5 mm	16×1.5 mm
Slice width		10.0 mm	5.0 mm/1.0 mm[b]	5.0 mm	5.0 mm
Feed/rotation	24 mm	–	24 mm	24 mm	24 mm
Pitch[c]	1.0	–	1.0	1.0	1.0
Rotation time	0.5 s	0.5 s	0.5 s	0.5 s	0.5 s
Increment	5.0 mm	–	5.0 mm 0.7 mm[b]	5.0 mm	5.0 mm
Start delay[a]	–	10 s	20 s	30–35s	60 s
Scan time[d]	5 s	–	5 s	5 s	5 s

[a]Alternatively, Automated Bolus Triggering (e.g., CARE Bolus)
[b]Reconstruction parameters for CT angiography
[c]Pitch=table speed per rotation/beam collimation
[d]Scan length=24 cm

more detector rows [6]. Depending on the manufacturer, the detector design varies substantially as shown in Table 2.

However, with regard to dose considerations, several general topics have to be considered in all types of MDCT scanners. First, the reconstruction of thin slices inherently generates more image noise, which may misguide the user to increase the radiation dose for compensation. However, spatial resolution improves linearly with reduction of the slice thickness whereas quantum noise just increases with the square root of the slice thickness ratio. Therefore, 3-mm-slice reconstruction has the potential to provide higher diagnostic confidence than 5-mm slices without need for dose compensation [10]. Secondly, despite the implementation of automatic dose control with tube current modulation in the latest scanners, MDCT of the abdomen generates a significant effective and organ-specific radiation dose in the patient. LiF-thermoluminescent-dosimeter measurements with an Alderson-Rando anthropomorphic phantom revealed a liver dose level of 21 mGy when a routine MDCT protocol was applied [11]. The corresponding effective dose in this study was approximately 13 mSv for a scan length of 42 cm. Although the cranio-caudal extension of the field of view can be lowered for focused liver examination, substantial radiation exposure remains, which is multiplied when multiphase series are applied. Thus, the number of necessary scans should be strictly checked for each patient with respect to the individual clinical question and history of the patient.

Benefits and limitations of MDCT in small focal liver lesions

The most impressive difference between SSCT and MDCT is the advance in scanning speed and reduction in slice thickness. For liver imaging, reduction of slice thickness mainly aims at improving the overall detection rate and characterization of small focal liver lesions that otherwise would have been missed or misinterpreted. In SSCT, a beam collimation of 5 mm and a pitch of 1.5 are commonly applied in order to attain an adequate slice thickness and radiation dose. Taking into consideration these parameters, partial volume effects and consecutive diagnostic misinterpretation become critical if lesion size drops to about 10 mm or lower. Here, the lower collimation width in MDCT has the potential to overcome the limitations of diagnostic assessment in small liver lesions.

However, two aspects have to be considered in MDCT imaging of very small liver lesions. First there are physical restrictions with special focus on X-ray dose saving. In MDCT, the X-ray beam cannot be completely utilized for diagnostic imaging, since the collimated dose profile is a trapezoid in the longitudinal direction, of which only the plateau part is usable for detector signal conversion, whereas the marginal portions form the "penumbra" and therefore imply a waste of dose. From that technological point of view, the relative contribution of the penumbral region increases with decreasing section width, and it decreases with increasing numbers of simultaneously acquired images [11]. Detection of very small liver lesions demands the application of the lowest beam collimation, implying a less efficient X-ray utilization with a decrease in signal-to-noise. However, to compensate for that unwanted effect, a disproportional increase in X-ray output would be necessary with a markedly elevated radiation dose.

Kopka et al. investigated the benefits and limitations of varying slice thickness in small liver lesion diagnosis and also applied a low 1-mm detector collimation. The authors reported that 2- and 4-mm slice reconstruction provided improved diagnostic results for assessment of small liver lesions sized 11 mm or less, yielding a detection rate and accuracy, respectively, of 96 and 87% at 4 mm and 96 and

84% at 2 mm [12]. Larger sections of 6, 8, and 10 mm yielded significantly inferior detections rates of 84, 75, and 70%, respectively, indicating that partial volume effects become more significant at lower z-axis resolution. However 1-mm slices also turned out to be inferior with a detection rate of 85%. Here, the benefit of high z-axis resolution and nearly isotropic CT imaging was obviously counteracted by the marked decrease in signal-to-noise ratio at lowest beam collimation. Haider et al. evaluated 88 liver lesions of less than 1.5 cm with 4-row MDCT comparing collimations from 2.5–5 mm with a 50% overlap of slice reconstruction [13]. In that study, pooled sensitivity for all lesions improved significantly as well with thinner collimation (66, 69, and 82% at collimations of 5.00, 3.75, and 2.50 mm). However, the authors also pointed out that image noise, being about twice as high in the 2.5-mm reconstructions, worsened the diagnostic confidence in the thinnest slice reconstructions.

Apart from the technological aspect, it is noteworthy that the prevalence of small benign liver lesions is substantial. Even in a preselected population of patients with known primary malignancy, the prevalence of malign focal liver lesions is rather low. The previously mentioned study of Haider et al. showed that 72% of liver lesions turned out to be of benign nature. In this respect, it is important to bear in mind that simple cysts can be found in up to 14% and hemangioma in up to 20% of the population [2, 14]. In a study of 2,978 patients with various common types of cancers, Schwartz et al. found small hepatic lesions in 12.7% of patients; these lesions were benign in 80% of patients and metastatic in 12% (according to stability at follow-up CT) [15]. Khalil et al. investigated a series of 1,012 patients with breast cancer and found at least one very small hepatic lesion in 29% of the women with no definite hepatic metastasis [16]. In 93–97% of the women without gross liver metastasis at presentation, the tiny hepatic lesions represented a benign finding. The authors discuss cysts, biliary hamartomas, and hemangiomas as the most likely differential diagnoses for single or multiple very small liver lesions. Robinson et al. investigated 115 patients with known or suspected malignant disease and found 79% of small indeterminate liver lesions to be stable in the follow-up examination indicating a benign nature. The authors concluded that the smaller the lesion, the less likely it was to be unstable [17]. These results again may reflect the finding that the likelihood the smaller a lesion detected with CT is, the more likely it is to be benign, probably due to the fact that the cysts and biliary hamartomas that represent a substantial proportion of these lesions basically provide a higher liver–lesion contrast than malign tumors do. The limitation of MDCT in diagnostics of small liver lesions therefore is on the one hand due to physical restrictions and the necessity of limiting X-ray doses in patient examinations, and on the other hand due to the high prevalence of benign small liver foci resulting in an increased number of accidental findings with an inherently low pretest probability of malign lesions.

Liver circulation and contrast application

Detection of liver lesions relies on creating images that provide optimum liver-to-tumor contrast. The conspicuity of pathologic lesions in native CT in general is rather low unless calcification or diffuse fatty infiltration of the surrounding parenchyma is present. Therefore, the use of iodinized contrast agents is essential. Since hepatic circulation is dominated by two major components, arterial and portal venous, bolus administration of contrast agent will lead to a typical two-phase enhancement: an initial visualization of the hepatic artery vessels followed by the portal venous inflow and opacification of hepatic parenchyma and liver veins.

Most liver tumors receive their blood supply from the hepatic artery, which nonetheless is a criterium for dignity [20]. However, the nature of focal liver lesions can be characterized by differences in the tumor vascularization pattern, which may be hypervascular, hypovascular or similar to normal liver tissue. CT appearance of different degrees of vascularity in liver lesions following bolus contrast application has been described by Foley et al. [21].

The first phase at approximately 20 s p.i. gives best contrast to the hepatic artery and its branches and thus is called the “early arterial phase” or “hepatic arterial phase.” Image acquisition during this phase is best for assessing the hepatic arterial anatomy but less sensitive for tumor detection. At 30–35 s p.i. portal venous inflow starts and is called the “portal venous inflow phase” or “late arterial phase.” At this point, opacification is still hepatic artery-dominant and liver attenuation is limited, which gives the best liver-to-tumor contrast in hypervascular focal lesions. Approximately 60 s p.i. the contrast material has arrived at the hepatic veins, hence this phase is called “hepatic venous phase.” Liver enhancement is maximum at this point as is liver-to-tumor contrast of hypovascular tumors. With a delay of approximately 2–3 min p.i., contrast-material equilibrium of the intravascular and extravascular components occurs [20]. This late phase is therefore called the “equilibrium phase” or “delayed phase,” and it may be suitable for demonstrating slow changes in tumoral enhancement as well as contrast-material pooling effects or typical fill-in patterns of hemangioma. However, in many instances attenuation differences between tumors and liver tissue disappear unless there is a larger mass or necrotic degeneration [20].

Contrast injection

The dynamics of the contrast enhancement are determined by cardiac output, injection rate, total volume of contrast

medium injected, concentration of the contrast medium and whether mono- versus biphasic injection protocol is applied [22]. The specific dynamics of contrast material application have been evaluated by Brink [23]. The authors point out the following key features:

1. The magnitude of hepatic tissue enhancement is related primarily to the total amount of iodinated contrast material that accumulates in the extravascular space of the liver.
2. The time-to-peak aortic enhancement is inversely correlated with the injection flow.
3. The magnitude of arterial enhancement increases with both the concentration and rate of contrast administration.

The main injection factor that influences arterial enhancement is the iodine flux, which can be influenced either by elevation of the delivery rate or concentration of the contrast material [25].

The peak hepatic enhancement is related to the total amount of iodinated contrast material traveling to the interstitial space of the liver parenchyma via the hepatic arteries and portal vein. This proportion can be maximized when CT is applied during arterial portography [25–28]. Though providing excellent images, this procedure is rather invasive and has been increasingly abandoned during recent years due to the increasing diagnostic potential of current MDCT and MRI devices. However, intravenous administration of contrast agent generally suffers from bypass flow through the aorta and subsequent proximal branches. The requirement for high-diagnostic-quality hepatic CT is maximum hepatic enhancement of at least 50 HU, which can be approached with a dose of 521 mg/kg iodine [26, 29]. This dose corresponds to 1.7 ml/kg of contrast material with an iodine concentration of 300 mg/ml or 1.4 ml/kg with an concentration of 370 mg/ml.

In order to circumvent pronounced dilution of intravenously administered contrast agent due to bypass flow, a rapid injection of the contrast agent is necessary for acquiring a satisfactory bolus formation and an appropriate enhancement of the hepatic vessels [25, 30]. The dynamics of iodine contrast material in liver CT have been thoroughly investigated by Awai and colleagues.

Awai et al. found in an Asian study population that the aortic peak time, the aortic peak enhancement, and the duration of aortic enhancement plateau in a monophasic injection procedure are related to body weight; the authors therefore advocate a fixed duration rather than a fixed flow of contrast agent injection [34]. Using iopamidol with an iodine concentration of 300 mg/ml, the authors compared two monophasic injection flows with an iodine flux of either 15 mg kg^{-1} s^{-1} (according to 3.6 ml/s at a body weight of 75 kg) or 20 mg kg^{-1} s^{-1} (according to 5.1 ml/s at a body weight of 75 kg). The higher flow resulted in a shorter mean aortic peak time of 21 versus 29 s, a higher mean aortic peak enhancement of 317 versus 269 HU and a shorter mean plateau time (HU greater than 200) of 21 versus 24 s [29].

However, favoring a body-weight-tailored contrast injection rate in a routine liver CT protocol requires an individual calculation of the injection rate for each patient, which may be annoying in daily use where standardized protocols usually are preferred. On the other hand, injection rates tailored to the body weight play a significant role in Asia, where the mean patient's weight usually does not exceed 60 kg. In the Western countries, where the patient's weight normally is at least 70 kg and obesity is a common finding, a fixed injection rate of 3–5 ml/s may usually be appropriate and a flow greater than 5 ml/s is less practicable since larger vein drains are needed and the risk of extravasation increases, particularly in patients with compromised peripheral vein conditions. Indeed, contrast injection using a standardized flow of 3–5 ml/s has been proven to provide a mean aortic enhancement of at least 150 HU and a mean peak hepatic enhancement of 63 HU [21].

Bae et al. supplied some additional data about contrast-agent dynamics, applying computer-aided simulation [22]. They found that with monophasic injection an increasing flow resulted in a shortening of aortic peak time, and higher contrast agent dose increased the peak level of aortic enhancement. Thus, a rapid injection of a high dose produced an early high peak enhancement whereas slow injection of less contrast material resulted in a flattened enhancement curve with delayed peak onset. In contrast, biphasic injection with a rapid initial flow, followed by a moderate second-phase injection rate, also reached a high aortic peak enhancement but lengthened the plateau period of the enhancement curve.

Foley et al. found in 109 patients that, with a monophasic injection rate of 3 ml/s versus a biphasic protocol of 5 ml/s for 10 s and 2 ml/s for 65 s, the aortic peak enhancement was higher and the time to equilibrium was slightly lower, but peak hepatic enhancement had been equally sufficient in attaining a level of about 64 HU [31].

A question arises as to whether high-concentration iodine contrast agent provides further improvement of liver CT enhancement. Roos et al. required a minimum iodine concentration of 300 mg/ml for sufficient liver enhancement [32]. Takada et al. investigated the influence of contrast-agent concentration and found that higher concentration is advantageous for imaging of arterial-dominant lesions [33]. Awai et al. investigated 92 patients with chronic liver damage using Iopamidol with a high iodine concentration of 370 mg/ml and an iodine flux of 20 mg kg^{-1} s^{-1}, corresoponding to 0.056 ml kg^{-1} s^{-1} [34]. With this setting, a mean peak aortic enhancement of 279 HU and a mean peak enhancement of liver parenchyma of 52 HU could be achieved, whereas the mean time to the maximum hepatic enhancement was 46 s. Yague et al. compared 370 mg/ml with 300 mg/ml iodine concentration applying four-phase MDCT in 100 consecutive patients, of

whom 27 had hypervascular HCC [35]. The authors found an iodine concentration of 370 mg/ml to be superior to 300 mg/ml with respect to the tumor-to-liver contrast in the late arterial phase and the peak hepatic enhancement. Awai et al. investigated iopamidol with an iodine concentration of 300 mg/ml versus 370 mg/ml, performing three-phase liver MDCT in 201 patients, of whom 58 had HCC [35]. The high-concentration contrast agent provided a gain in the peak aortic enhancement of about 14% and in the arterial-phase tumor-to-liver contrast of about 50%. However, in a more recent study, Awai et al. found deviating results in which administration of iohexol with an iodine concentration of 300 mg/ml versus 350 mg/ml yielded a significantly higher aortic enhancement during all four MDCT phases in 186 patients and also significantly better late-arterial tumor-to-liver contrast in 67 patients with hypervascular HCC, whereas hepatic enhancement was similar in the hepatic vein phase and during equilibrium [37]. The reason for these ambiguous results is probably a partial loss of the contrast bolus in the "dead space" between the brachial vein and the superior vena cava, where about 20–30 ml of contrast material can be retained [38]. In order to avoid this unwanted effect, a saline chaser is helpful for pushing the contrast material bolus via the venous vessels forward to the aorta and hepatic artery.

By these means, Tatsugami et al. found a significantly higher enhancement value of the abdominal aorta, portal vein, and liver parenchyma in 108 patients when they used a 50 ml saline chaser in addition to administration of 100 ml Iomeprol [39]. Dorio et al. successfully applied a saline chaser of 50 ml in 26 patients with 86 hypoattenuating liver metastases to lower the total amount of contrast agent to 100 from 150 ml with no relevant decrease in image quality; they propose the saline flush as a suitable means for decreasing examination costs and risk of nephropathy [40].

At our institute, we prefer a biphasic injection procedure with initial administration of 80 ml contrast solution (370 mg/ml iodine) at a flow rate of 3.5 ml/s, followed by 50 ml contrast agent at a flow rate of 1.5 ml/s and a saline chaser of 50 ml at a flow rate of 2.5 ml/s.

The capability of MDCT scanners to perform a liver scan in under 10 s providing sharply separated multiphase perfusion images requires that the start delay of the scan is accurately adapted to the bolus injection of the contrast agent. In multiphase MDCT, the portal venous phase is longer, whereas the arterial phase is relatively brief, which makes optimal timing of the arterial phase most critical. However, the question of whether a fixed time delay, a timing bolus or an automatic bolus tracking method should be applied is still discussed controversially. For fixed time delay, the scan should be started at 25–35 s for the late arterial phase and 60 s for the hepatic vein phase [20, 52]. However, as mentioned above, particularly in patients with cardiac disorders, the circulation time may vary significantly. Sandstede et al. investigated 150 gender- and age-matched patients and found a remarkable interindividual variation in peak transit time with a range of 10–30 s, indicating that individual timing may be advisable [41]. Itoh et al. on the other hand, found no differences in image quality and liver enhancement when comparing a fixed delay of 30 s and automated bolus trigger method [42]. Nevertheless, if individual timing delay is intended, the arrival time of the main bolus can either be determined with a timing bolus or an automated tracking procedure. Using a timing bolus requires an accessory measurement with injection of a mini-contrast bolus of 10–20 ml; after that, a single-level serial low-dose CT (120 kV, 20 mAs, cycle time: 2 s, start delay 10 s) is applied. From a region of interest within the aorta on the level of the celiac artery, a time–signal curve can be acquired that reveals the time-to-peak aortic enhancement as optimal delay time for the subsequent liver examination [36, 43].

Alternatively, semi-automated timing protocols are available (e.g., CARE Bolus, Siemens Medical Solution, Erlangen, Germany), which trigger liver scanning by means of a preceding low-dose time-resolved acquisition and ROI measurement on the aortic level of the celiac artery. The advantage of the latter procedure is reduction in contrast agent and examination time and easy-to-use protocol setting. Furthermore, a timing bolus, though not necessarily requiring a greater amount of iodine content, will leave some residual iodine contamination in the area of interest, which impairs the contrast conditions of the subsequent liver study.

At our institute we favor the semi-automated trigger procedure, which implements real-time display serial CT of the aorta at the level of the celiac artery, and allows for manual user-defined scan initiation, which is advantageous in patients with compromised cardiac output and slow and uncertain aortic signal up-slope. If manual interaction is not used, the scan procedure is automatically triggered as soon as an aortic threshold of 150 HU is reached. The delay for automated scan initiation is set to 8 s and comprises rapid table movement towards the predefined start position for the first liver scan followed by a recorded breathing command message; the helical scan starts instantly afterwards for the late arterial phase. With a further delay of 40 s, the hepatic vein phase is acquired in the same manner.

If initial finding of dual-phase scanning is ambiguous, a late phase after 3–5 min may be added in order to better characterize the nature of a detected lesion, e.g., in suspected hemangioma.

Multiphase imaging

MDCT diagnostics of focal liver lesions requires high-spatial-resolution imaging of the dynamic density characteristics during iodine contrast-material transit reflecting the perfusion and vascularization pattern of the underlying tissue pathology. Therefore, at least dual-phase bolus

contrast-enhanced MDCT with 5-mm-slice reconstruction is needed [44, 45]. Precontrast scan is advisable in the baseline CT examination but may be abandoned in follow-up study in order to limit the radiation exposure. Delayed CT scans should be restricted to those cases where no conclusive perfusion pattern is exhibited in the dual-phase contrast series. The acquisition of an arterial dominant perfusion scan is crucial, since approximately 30% of the lesions are detectable exclusively on the arterial phase images (Fig. 1) [20, 46]. Hypervascular lesions are best seen in the late arterial phase, during which the contrast material reaches the peak enhancement of the arterial tumor neovasculature [20, 21]. However, study data investigating patients with hepatocellular carcinomas indicate that triple-pass CT is slightly but significantly superior to dual-phase imaging in terms of lesion detection and characterization [20, 47]. In contrast, Murakami et al. concede that the early arterial phase may be abandoned as long as correct bolus timing is ensured [48]. These data are supported by Francis and colleagues, who found no improved tumor conspicuity by either quantitative or subjective analysis in 52 patients [49]. However, early arterial phase imaging provides the best enhancement of the arterial hepatic vessels and therefore is preferable to CT arteriography and 3D reconstruction [50]. Also, the early arterial phase is best for detection of arterial-portal venous shunts, which inherently present a time-to-peak enhancement similar to that of the hepatic artery supply. The liver-to-tumor contrast and thus the detectability of hypovascular lesions, particularly metastases, is highest during the hepatic vein phase when enhancement of the liver parenchyma reaches its maximum [51, 52].

MDCT of benign focal liver lesions

The liver is the lynchpin of body metabolism, with excretory, intake and immunologic functions and is a major part of blood circulation. Thus, the liver may be affected by a large variety of diseases and pathologic alterations either of primary or secondary origin. Though substantially differing in occurence, basically all main components of the liver tissue (hepatocytes, biliary epithelium, mesenchymal tissue) can give rise to both benign and malign tumors (Table 4).

Due to the complexity of liver disease, imaging, even at its best, will often be only one part of a diagnostic puzzle; consideration of concomitant findings such as specific laboratory abnormalities; history of infection, toxic exposure or hemochromatosis; and underlying systemic diseases or known malignancies will be crucial for final diagnosis. Taking into account the broad prevalence and incidence of focal liver changes, clinical imaging and differential diagnosis should primarily focus on the most common entities and thereafter will have to consider the more rare entities. By far the most common entity is hemangioma with a prevalence of 2–20% [2, 53] followed far behind by focal nodular hyperplasia (FNH), and liver adenoma, which is a rather rare entity. Due to the high prevalence of benign tumors, MDCT of the liver is challenging in terms of distinguishing benign lesions, which in most instances can be left alone, from malign neoplasms requiring therapy. From a practical point of view confident diagnosis of hemangioma and FNH resolves 90% of all focal benign liver lesions [52]. However, liver adenoma has to be excluded, since, although being benign, it often is a candidate for surgical resection due to the risk of bleeding and malign transformation. A condition of particular note is preexisting liver

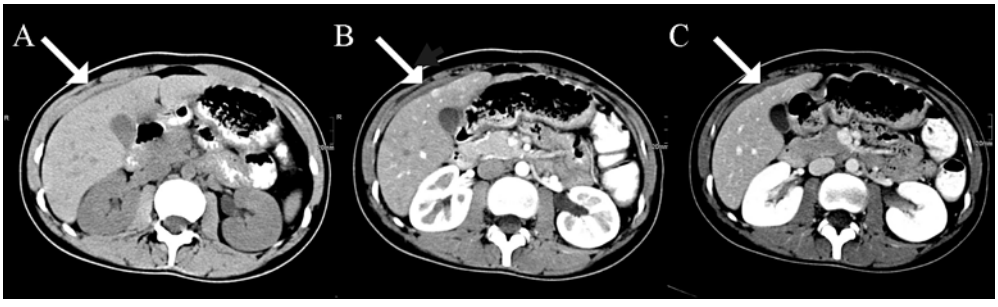

Fig. 1a–c Example of a small-sized lesion <1 cm with ambigous appearance on multiphase MDCT of a 19-year-old male patient with upper abdomen pain (*white arrows*). At the ventral paramedian margin of the liver, a very tiny lesion is seen, which slightly bulges out the liver surface and shows a transient uniform enhancement in the late arterial phase (**b**) but is not visible on the precontrast (**a**) and hepatic vein scan (**c**). No final diagnosis could be made on basis of the CT examination and no further imaging (MRI, scintigraphy, ce-ultrasound) was available. The main differential diagnosis includes HCA, FNH, regenerative nodule, HCC and hypervascular metastatic tumor. However, this subtle finding underlines the importance of proper contrast-enhancement during multiphase MDCT. MDCT was performed with a 4-detector scanner (SOMATOM Volume Zoom, Siemens Medical Systems, Erlangen, Germany) using 4×2.5 detector collimation with 155 effective mAs and 120 KV radiation exposure. Biphasic bolus administration of 130 ml Iopromid (370 mg iodine/ml) with saline chaser and automated scan triggering was obtained. On the basis of 5 mm continous axial slice reconstructions region-of-interest density measurements in precontrast/late arterial/portal vein scan yieleded within the abdominal aorta 43/287/187 HU and within the hepatic tissue 67/99/132 HU. Maximum enhancement within the lesion was 153 HU during the late arterial phase corresponding to a liver-to-tumor contrast of 64 HU

Table 4 Primary benign focal liver neoplasms and malign analogues by histologic origin (common abbreviations are given *in parenthesis*)

	Benign	Malign
Hepatocyte origin	Hepatocellular adenoma (HCA)	Hepatocellular carcinoma (HCC)
	Adenomatous hyperplastic nodule (AHN)	
	Focal nodular hyperplasia (FNH)	Fibrolamellar carcinoma (FLC)
Biliary origin	Cystadenom	Cystadenocarcinoma
	Simple cyst	Cholangiocarcinoma (CAC)
	Biliary hamartoma	
Mesenchymal origin	Hemangioma	Angiosarcoma
	Hemangioendothelioma	
		Mesenchymal sarcomas:
		Angiomyosarcoma
	Lipomatous tumors	Leiomyosarcoma
	Mesenchymal hamartoma	Rhabdomyosarcoma
		Fibrous sarcoma
		Malignant fibrous histiocytoma

cirrhosis. The diffuse pathologic changes of the hepatic architecture often induce an inhomogeneous appearance on contrast-enhanced CT due to alteration of arterial and portal venous liver circulation. Due to the increased incidence of HCC in cirrhotic liver, exclusion or detection of HCC is a challenging basic diagnostic problem. However, Freeny et al. studied explanted livers that had been imaged in vivo with CT prior to surgery for the presence of HCC. The authors found that 41 of 61 hypervascular lesions were regenerative nodules (RN), 3 of 61 were dysplastic nodules (DN), and 17 of 61 turned out to be HCC. Most RN/DP nodules were 5–20 mm in diameter, had distinct margins, were homogeneous, and were isoattenuating on precontrast, portal, and delayed scans. HCC nodules tended to be larger, approximately 6–50 mm. All showed positive contrast enhancement and displayed a wide range of attenuation profiles [54].

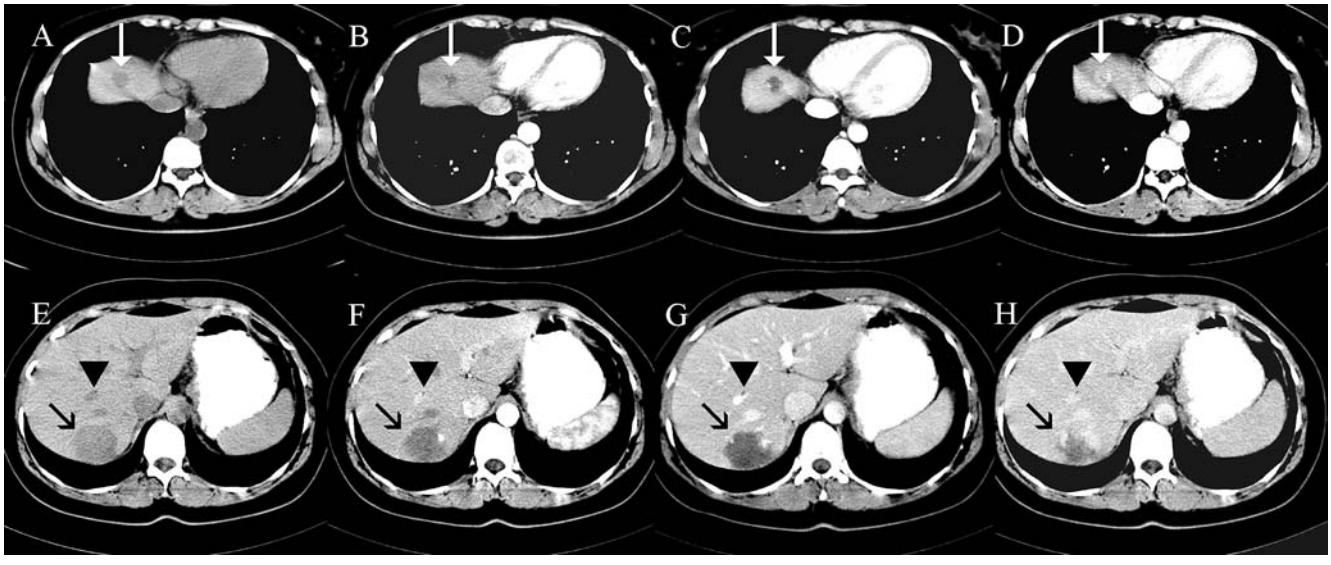

Fig. 2 Multiple liver lesions in a 31-year-old male patient. Multiphase MDCT demonstrated a small hemangioma in the right dome of liver (*white arrows*) with well-defined hypodense appearance on precontrast scan (**a**), slight globular peripheral enhancement but otherwise poor liver-to-tumor contrast in the late arterial phase (**b**), increasing peripheral hyperattenuation and central hypodense appearance in the hepatic vein phase (**c**) and nearly complete fill-in during equilibrium (**d**). A larger hemangioma in the dorsal aspect of the right liver lobe (*black arrows*) shows a similar density and enhancement pattern (**e**–**h**), although due to it's size, the centripetally advancing contrast enhancement is not yet terminated in the delayed scan (**h**). A further tiny hypodense lesion adjacent to a segmental branch of the right portal vein (*arrowheads*) exhibits hypoattenuation in all perfusion phases with no significant contrast material uptake and therefore was rated as a small cyst

Hemangioma

Hemangioma is a hamartoma that consists microscopically of multiple vascular channels lined by a single layer of endothelial cells and a thin fibrous stroma [14]. It accounts for 78% of all benign liver neoplasms and is the second most frequent lesion behind metastases [55]. The lesions are preferentially found in women, particularly postmenopausal women, with a F:M ratio of 5:1; hepatic hemangiomas in the childhood are rare [2, 56, 57, 63]. Depending on size and tissue architecture, fibrosis, hyalinization, and cystic changes may be present [60]. Due to a slow-flow situation, thrombosis of vascular channels is quite a common event resulting in fibrosis and calcifications [5, 58]. Hemangiomas may be multiple in up to 50% of cases (Fig. 2) [59]. Size can range from a few millimeters to more than 20 cm with lesions bigger than 10 cm usually defined as "giant hemangiomas." Rarely, adjacent abnormalities may be observed as arterial-portal venous shunts, capsular retraction, and surrounding nodular hyperplasia [60]. Furthermore, associated lesions may be present comprising multiple hemangiomas, hemangiomatosis, focal nodular hyperplasia, and angiosarcoma [60]. Complications consist of inflammation, Kasabach-Merritt syndrome, intratumoral hemorrhage, hemoperitoneum, volvulus, and compression of adjacent structures [60]. Since 85% of these lesions are asymptomatic, findings are mostly incidental during imaging of the upper abdomen. Generally, hemangioma is a favorite application for MRI, since very characteristic, marked T2 hyperintensity is present.

CT features of hemangioma are also characteristic and have been comprehensively studied in the era of single-slice CT, including appearance in multiphase imaging following contrast application. In most cases image findings will be typical, allowing for certain diagnosis with CT as well as with MRI. However, due to the relatively high prevalence of hepatic hemangioma, the radiologists may have to consider atypical CT appearance of hemangioma in some cases, which can involve a broad variety of different diagnoses; in some cases all imaging approaches may be inconclusive, and definite diagnosis has to be made by biopsy or surgical resection. Surgical intervention is also necessary in the rare instances of complicated hemangioma arising from inflammation, coagulation, hemorrhage with possible hemoperitoneum, volvulus, or compression of adjacent structures [60].

On unenhanced CT scans, the typical hemangioma shows well-defined, lobulated borders presenting near isoattenuation with blood and calcifications in 10–20% of the cases [58]. In dual-phase contrast CT, initial peripheral globular enhancement similar to that in the aorta is a very specific finding that can be seen in 67% of the cases [68]. In 10%, an additional central enhancement may be present [61]. Approximately 80–85% of hemangiomas show the

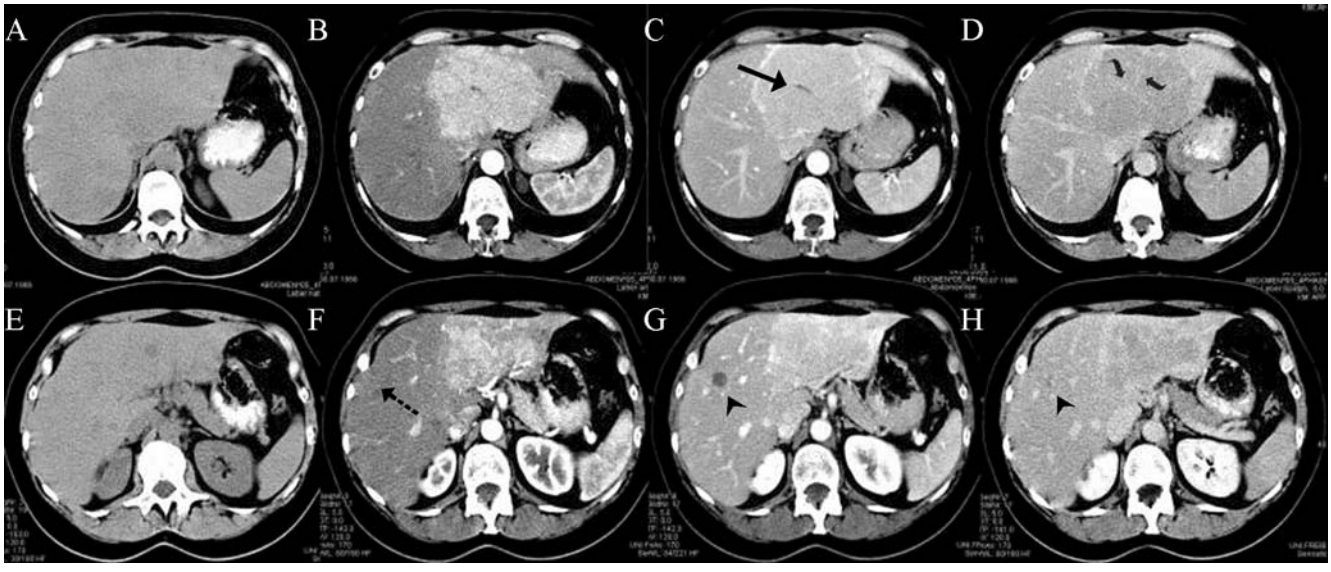

Fig. 3a–h Focal nodular hyperplasia with associated hemangioma in the same patient. Triple-phase MDCT liver study with precontrast scan at two anatomic levels. *Upper image series* shows the center of a large space-occupying FNH in the left liver lobe with slight hypoattenuation on precontrast scan (**a**), rapid homogeneous enhancement in the late arterial phase with demarcation of a central scar (**b**), persisting but decreasing hyperdensity in the hepatic vein phase where the central scar clearly can be delineated (*arrow*). Late scan in the equilibrium phase shows overall isoattenuation to the liver parenchyma with delayed enhancement of the central scar and associated fibrous bands (**d**, *curved arrows*). *Lower image series* displays a smaller hemangioma in the right liver lobe with isoattenuation on precontrast scan (**e**). In the late arterial phase, very discrete nodular central enhancement is present (**f**, *dashed arrow*) whereas the hepatic vein phase and scan during equilibrium show the typical centripetal "fill-in" enhancement pattern (**g**, **h**, *arrowheads*)

characteristic finding of initial nodular enhancement progressing centripetally, the "fill-in" pattern (Fig. 3) [62].

Atypical MDCT appearance of hemangioma may either result from deviant histopathology including hyalinization, fibrosis, thrombosis, calcification and scar-like compounds or be due instead to the size of the lesion [60]. In up to 15–20% of the cases, particularly with giant hemangioma, even on delayed scans a complete fill-in with central enhancement is missing and can likely be attributed to central fibrosis, thrombosis or scars [63]. On the other hand, the rapid filling that occurs in 16% of all hemangiomas can predominantly be found in small lesions and has been observed in 42% of hemangiomas less than 1 cm in diameter (Fig. 4) [60, 64]. In these cases, hypervascular hepatic or metastatic malign tumors may be considered as a differential diagnosis, but the typically persistent contrast enhancement of even small hemangiomas that are missing a wash-out phenomenon in the equilibrium phase is helpful for final diagnosis. Furthermore, small hemangiomas may exhibit arterio-venous shunting in up to 21% of cases [65]. Arterio-portal venous shunting in hemangiomas is usually asymptomatic and must not be misunderstood as a definitive sign of malignancy. However, since this finding is well-known in HCC, further diagnostics are usually performed and if an additional MRI is not conclusive, fine-needle biopsy should be considered [60, 66].

All imaging features of a hemangioma, provided its size is not minor, can usually be sufficiently demonstrated with single-slice CT. Since the perfusion characteristics of hemangioma result in slow enhancement pattern, the use of additional early phase scans has little chance of providing further diagnostic information. The benefit of MDCT may be to better characterize smaller subcapsulary localized lesions where partial volume effects can be reduced due to higher spatial resolution. Higher spatial resolution may also be beneficial for small hemangiomas, which often lack typical imaging features [67]. As with any other liver tumor mass, the capacity to produce high-quality non-axial reformations makes MDCT favorable for better imaging of the tumor site (e.g., pedunculated location) and its relationship to the surrounding tissue and organs.

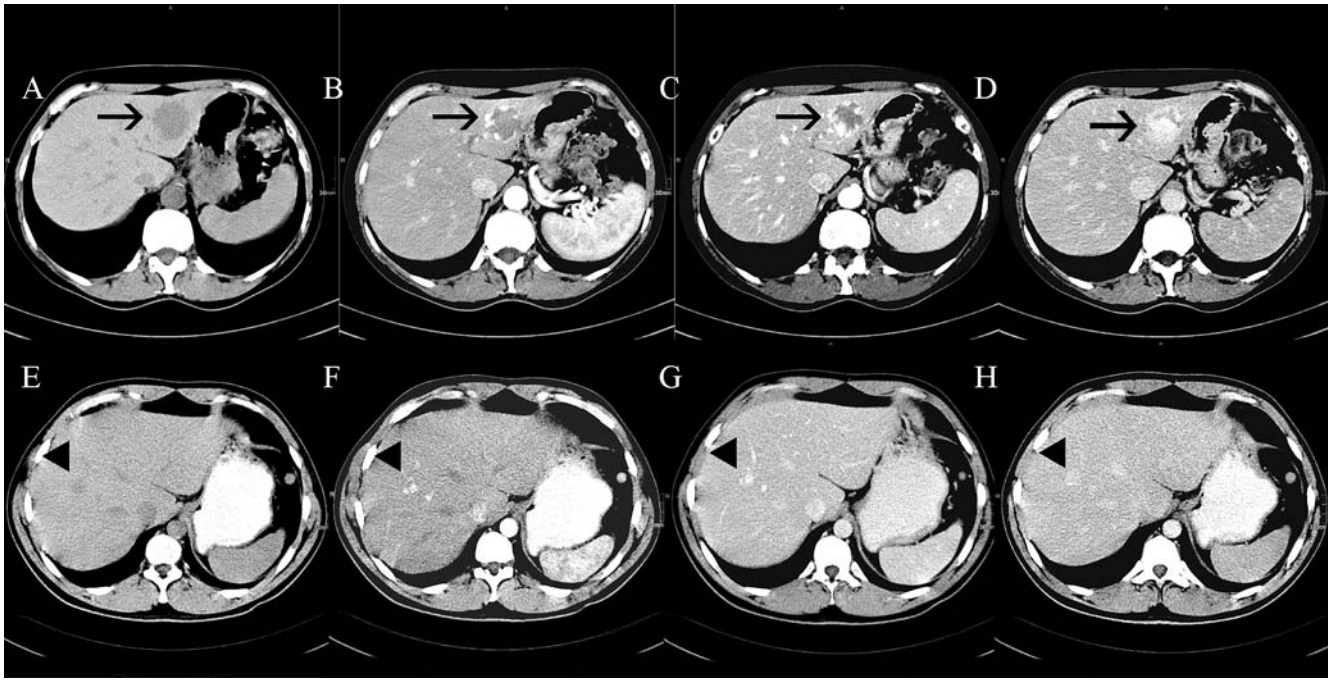

Fig. 4a–h Variably sized hemangiomas in two patients. The *upper row* shows typical multiphase CT appearance of an intermediate-sized hemangioma in a 64-year-old female who presented for assessment of an uncertain mass in the liver on ultrasound. A multiphase CT image series displays a well-defined lesion in the left lobe (*arrows*) with blood-equivalent hypoattenuation on precontrast scan (**a**). In the late arterial phase, marked globular peripheral enhancement is seen (**b**) with centripetally advancing enhancement in the hepatic vein phase (**c**) and nearly complete fill-in during equilibrium (**d**). The *bottom row* shows small-sized hemangioma in an 22-year-old male with chronic HCV infection, where MDCT was performed to exclude HCC. Multiphase imaging displays a hypodense lesion in the centrical right lobe of the liver with blood-like attenuation on precontrast scan (**e**). In the late arterial phase, spotty globular but marked enhancement is seen at the margins of the lesions (**f**). Due to the smaller size of the hemangioma, centripetally advancing enhancement occurs more rapidly than in the larger mass described above, with almost complete fill-in during the hepatic vein phase (**g**) and lower contrast on the delayed scan (**h**), where the lesion may be confused with hepatic vessels on superficial image reading

Focal nodular hyperplasia (FNH)

Focal nodular hyperplasia (FNH) is a rare tumor-like lesion twice as common as hepatic adenoma and mostly found in women in their third to fifth decades, with a F:M ratio of 2–4:1 and no definitive association with oral contraceptives. However, contraceptives seem to increase the rate of complications and to induce tumor growth [68]. It is assumed that FNH is a congenital hamartomatous malformation or reparative process that develops as a hyperplastic response to an underlying congenital arteriovenous malformation. Thus it presents microscopally as a central fibrous scar with surrounding nodules of hyperplastic hepatocytes and small bile ducts; central veins and portal triads are missing [14, 55]. FNH is usually smaller than 5 cm with a mean diameter of 3 cm at time of diagnosis [59]. The lesion appears as a well-circumscribed nonencapsulated nodular cirrhotic-like mass in an otherwise normal liver with absence of calcifications, bleeding, or necrosis [55]. The right lobe is preferentially affected; FNH may be pedunculated in 5–20% of cases and multiple in 20%. Patients with FNH display an increased rate of other vascular abnormalities such as teleangiectasia or arteriovenous malformation [69]. In 23% of cases, FNH is associated with hemangioma (Fig. 5) [70].

On CT prior to contrast injection, FNH is usually homogeneous and isoattenuating to liver parenchyma with no evidence of calcification. During the late arterial phase, rapid enhancement is displayed with demarcation of a hypodense central scar in 30% of cases [71]. The lesion is usually delineated by well-defined lobulated margins but no capsule. In the hepatic vein phase, FNH becomes isoattenuating to the liver tissue and may be difficult to detect (Figs. 3, 6). Late scans may show delayed enhancement of the central scar and optional fibrous septas as a quite specific feature [62].

If all characteristic imaging features are present, diagnosis may be quite confident with CT. However, typical appearance is missing in almost 50% of the lesions, especially those of smaller size [59]. Often the specific finding and contrast behavior of the central scar and the fine fibrous bands can not be observed. In these cases, other possible hypervascular malign tumor entities have to be considered and excluded.

MRI, in contrast, gives valuable additional information about the lesion's nature since it displays more the isoappearance with normal liver tissue and the fibrous content of the septas and scar components, with contrast dynamics similar to CT. The application of liver-specific contrast agent helps greatly in narrowing the differential diagnosis. With use of SPIO and USPIO, a marked loss of signal intensity can be observed that is greater than in other liver lesions such as hepatocellular adenoma [72]. With hepatobiliary contrast agents, the presence of hepatocytes within the lesion with contrast uptake and resulting hyperintensity compared to liver parenchyma can be demonstrated [73]. A recent study by Grazioli et al. demonstrates that delayed gadolinium–dimeglumine-enhanced MRI is an excellent diagnostic tool for distinction between FNH and HCA/liver adenomatosis compared to perfusion study [74]. One important differential diagnosis may be fibrolamellar carcinoma. If MRI is uncertain regarding this finding, on the other hand, CT is beneficial for detection of calcifications, which usually exclude FNH and make fibrolamellar carcinoma a likely alternative diagnosis.

MDCT is advantageous, since accurate multiphase scanning is necessary for final diagnosis of FNH. Although triple-pass imaging may not be necessary, thin-slice reconstructions can be helpful for detecting septas or scar components while providing more definite assessment of attenuation values due to decreased partial volume effects.

Even if the histopathology is challenging, in atypical FNH the patient has to undergo needle biopsy for definite diagnosis. Combined with imaging finding, this procedure clarifies 90% of the cases avoiding unnecessary surgery [75].

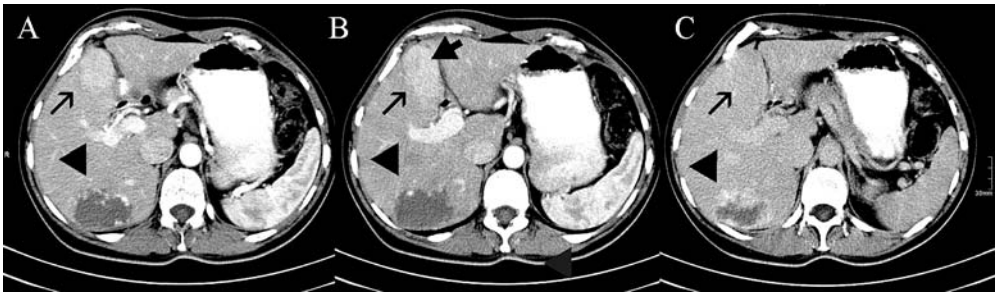

Fig. 5a–c Multiple liver lesions in a 51-year-old female patient. Contrast-enhanced MDCT of the liver where **a** and **b** shows two neighboring levels at the late arterial phase and **c** displays the hepatic vein phase at the anatomical level corresponding to **b**. An intermediate-sized hemangioma is visible in the dorsal aspect of the right lobe with typical globular peripheral enhancement in the late arterial phase and advancing fill-in during the hepatic vein phase (*arrowheads*). In the ventral aspect of the liver, a second lesion exhibits expansive appearance with marked transient homogeneous enhancement in the late arterial phase and isoattenuation in the hepatic vein phase (*black long arrows*). A tiny central scar is visible solely at one slice position (**b**, *black short arrow*) during the arterial dominant phase, matching the histology of an FNH

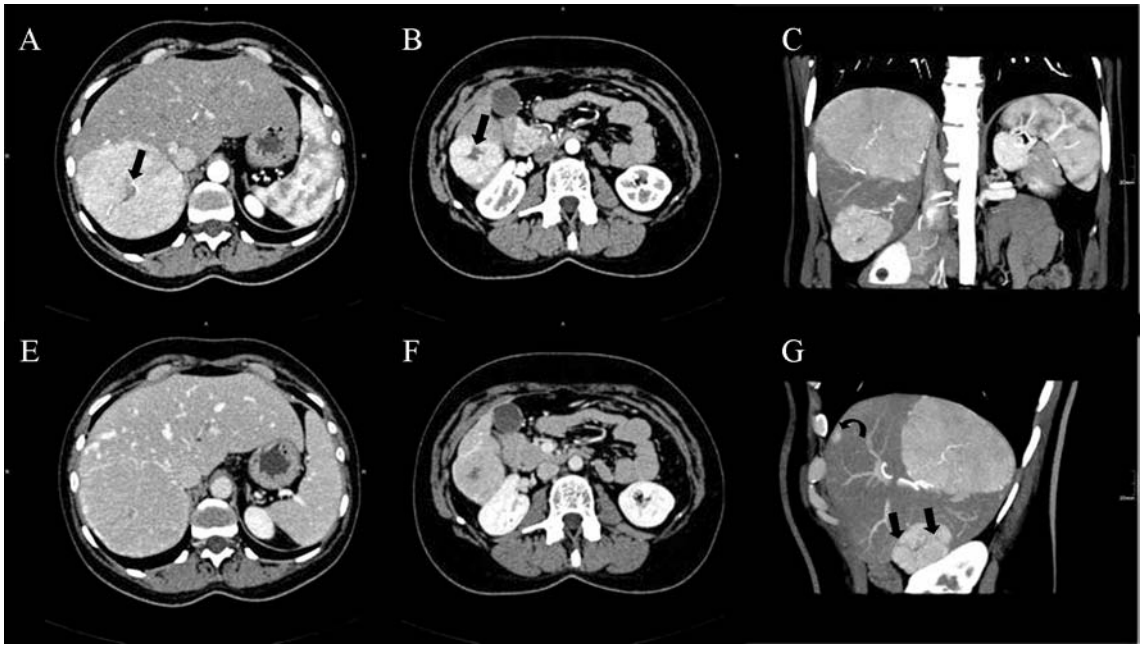

Fig. 6a–g Multifocal focal nodular hyperplasia in a 40-year-old female patient. Multiphase MDCT shows two slightly lobulated hypervascular tumors in the right lobe of the liver with marked enhancement in the late arterial phase (**a**, **b**) and evidence of a typical central scar within the lesions (*arrows*). The late arterial phase demonstrates isoattenuation to the normal liver parenchyma (**e**, **f**). Thin-slice maximum-intensity projections from the late arterial phase of the same data set provide a good impression of the tumor site with respect to the surrounding tissue and margins of the liver (**c**, **g**). Additionally, small fibrous septas are visible within the lower lesion (**g**, *straight arrows*) and a further subcapsulary small hypervascular adenoma can be seen adjacent to the anterior liver margin (**g**, *curved arrow*)

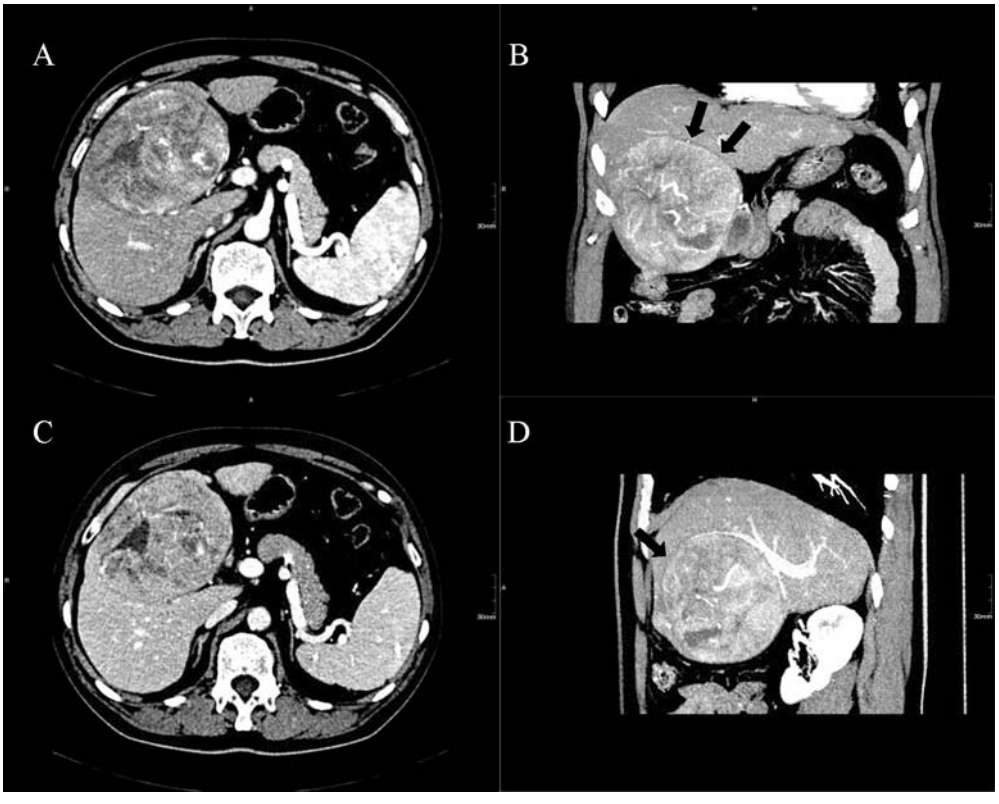

Fig. 7a–d Hepatic adenoma in a 60-year-old male patient. Multiphase MDCT demonstrates a large well-defined inhomogeneous mass in the anterior right lobe of the liver with multifocal areas of necrosis and large arterial tumor vessels. The late arterial phase (**a**) shows moderate enhancement with isoattenuation in the hepatic inflow phase (**c**). Coronal (**b**) and sagittal (**d**) thin-slice maximum-intensity projection from the late arterial phase of the same data set nicely displays the site of the tumor bulging out the lower margin of the liver and displacing the adjacent portal veins. Again large tumor vessels from the hepatic artery supply are seen within the lesion (**b**) including the pseudo-capsule (*arrows*)

Hepatocellular adenoma (HCA)

Hepatocellular adenoma (HCA) is a rare primary liver tumor consisting of hepatocytes with increased glycogen and fat content arranged in cords with no portal or central hepatic veins. Bile ducts are not functional, and Kupffer cells are demonstrable within the tumor [5]. The tumor is commonly delineated by a pseudocapsule from which the vascular supply arises centripetally via peripheral hepatic arterial feeding vessels. HCA is solitary in 80% of cases but also can be multiple (more than four lesions), with a mean diameter of 8–10 cm at discovery; subcapsulary localization is common and pedunculation is found in 10% of cases [14, 58]. Oral contraceptives and androgen steroid therapy have been definitely proven to be causative agents. This is why the majority of HCA cases are found in younger women using oral contraceptives, and the incidence of the disease has markedly increased with the widespread use of these medications [59]. Withdrawal of estrogen compounds may lead to regression of existing HCA. Although most of the tumors are asymptomatic, there is a significant danger of rupture and consequent internal bleeding. Furthermore, the potential of malignant transformation has to be considered. That is why, contrary to FNH, HCA is treated more aggressively and preferentially resected surgically.

On unenhanced CT, HCA is rather well-confined with inhomogeneous appearance due to fat content or necrosis, fresher hemorrhages can also result in hyperattenuation. Following bolus contrast injection, there is early enhancement in the late arterial phase, which may be homogeneous in smaller lesions. In larger tumors, a centripetal enhancement pattern starting from the subcapsulary feeding vessels may be seen with persistent hypodense areas due to necrosis or fat and glycogen content [59]. Enhancement is rather transient because of arterio-venous shunting, lowering the liver-to-tumor contrast in the hepatic vein phase (Fig. 7) [76].

Ruppert-Kohlmayr et al. found the relative enhancement of FNH in the early arterial phase (20 s p.i.) to be significantly higher than in HCA whereas results in unenhanced scans and the hepatic vein phase were ambiguous [77]. Using a 1.6 cut-off for relative enhancement in the early arterial phase provided an accuracy of 96%. Although typical findings such as subcapsulary feeding vessels with centripetal enhancement in HCA and central scar with centrifugal enhancement in FNH were less common in smaller lesions (<3 cm), measurement of attenuation values still was found to be helpful and distinction between HCA and FNH also applicable. These findings are promising but still have not been supported by larger studies.

The larger the tumor the more likely is the presence of typical findings for HCA as well as FNH. Difficulties may remain in small lesions where the specific patterns become less clear. In these cases, with MDCT, thin slices of 3 cm or less can be reconstructed with accurate separation of each perfusion phase. Although the image appearance of tumors of hepatic origin such as HCA, FNH, and HCC tend to become more ambiguous the smaller the lesion is, better temporal and spatial resolution basically promises higher detection rates as well as more reliable Hounsfield contrast due to reduced partial volume effects [20]. To what extent this feature contributes to a relevant advance in diagnostics with respect to clinical demands, therapeutic implications, and outcome still has to be investigated in larger study populations. As of now, no study data have proved a substantial improvement in diagnostic accuracy by increasing the number of detector rows beyond 16.

Even with MDCT the distinction between HCA and low-grade hepatocellular carcinoma is still challenging. A breakthrough advance can not be expected using the multidetector scanners, since the imaging patterns of both entities relating to morphology and perfusion pattern inherently show an ambiguous overlap, making certain detection or exclusion of malignancy impossible in many cases.

Conclusion

MDCT is a rapidly evolving technique that significantly improves CT imaging for several indications. Whereas initial systems featured 4 detector rows the latest scanner types provide up to 64 rows providing the capability of true isotropic data acquisition. This results particularly in improved longitudinal spatial resolution allowing high-quality nonaxial reformations and 3D reconstructions. Visualization of normal anatomy, as well as any pathologic changes and the relationship to surrounding structures becomes more plastic, facilitating morphologic assessment in clinical practice.

Additionally, MDCT scanning time has dramatically decreased allowing rapid accurate multiphasic imaging with short breath-holding periods. The combination of MDCT and the optimization of contrast-agent administration has significantly improved the quality of multiphasic liver imaging with respect to accurate depiction of perfusion as well as through-plane resolution. The detection rate of small lesions profits from thinner slices. The capability to acquire early arterial images with thin collimation makes high-quality CT angiography possible, which is advantageous in presurgical evaluation as is any other high-resolution 3D reformation.

Apart from this, it has, however, not been clearly proven that MDCT is superior to helical single-slice CT for assessment of benign focal liver lesions. From a clinical point of view, the main question arises as to whether a liver lesion should be resected or not. For this reason, confident differentiation of HCA from hemangioma and FNH may be considered sufficient. Sparse data exist that the capacity to acquire an early arterial phase improves the distinction

between FNH and HCA, but this conclusion surely must be supported by further investigations. Whereas large tumors exhibit typical patterns of morphology, attenuation and perfusion, small lesions still remain challenging even with MDCT, since the specific criteria for confident diagnosis become more ambiguous. In this respect the distinction between HCA and hepatocellular carcinoma still remains uncertain due to an inherent overlap of CT appearance among these entities.

Due to its low costs and widespread availability, ultrasound (US) always has to be taken into consideration for diagnosing focal liver lesions. Compared with conventional B-mode gray-scale US, significant advantages arise from the additional use of color Doppler and power modes with respect to the evaluation of tumor vascularity [78]. However, despite recent improvements in color Doppler sonographic equipment, conventional color Doppler is still limited by its lack of sensitivity in the detection of flow in intranodular microvessels or flow in deeply located liver lesions, and the examination procedure is hampered by motion artifacts (heartbeat, breath) [78].

Nevertheless, developments in ultrasound with contrast-enhanced pulse-inversion technique provide increasing competition to MDCT and MRI, since high-temporal-resolution multiphase imaging displaying the micro- and macrovasculature of a liver lesion provides an additional clue to final diagnosis [79]. With the administration of second-generation microbubble preparations, an extended time window can be utilized for continuous multiphase scanning of the entire liver and imaging the perfusion feature of a focal lesion with cine-loops of the acquired raw data. With the use of all modalities of ultrasound (gray-scale sonography, conventional color Doppler and contrast-enhanced color Doppler), a valid diagnosis of a focal liver lesion can be made possible in up to 79% of the cases [78]. However, the authors, acknowledging a multi-reader study evaluation, admit that only the FNHs could be clearly distinguished from malignant tumors. All other lesions could not be characterized distinctly, and a definite differentiation between benign and malign diagnosis in particular could not be achieved.

MRI in contrast provides further and more detailed information about tissue components than MDCT and has also experienced a great evolution in recent years, which makes this technique still the standard of reference for evaluation of focal liver lesions. The additional use of liver-specific contrast agents adds further efficacy. A recent study by Grazioli et al. demonstrated that delayed gadolinium–dimeglumine-enhanced MRI is a more reliable diagnostic tool for distinction between FNH and HCA/liver adenomatosis than perfusion study [74]. Additional studies are needed in order to decide whether the latest MDCT scanner types in combination with novel management of contrast application provide clinically relevant information for assessment of benign focal liver lesions. Finally, MDCT of the abdomen generates a significant and organ-specific radiation dose to the patient. Thus, the number of necessary scans as well as the application of lower collimation should be strictly checked for each patient with respect to the individual clinical question and history of the patient.

References

1. Fox SH, Tanenbaum LN, Ackelsberg S et al (1998) Future directions in CT technology. Neuroimaging Clin North Am 8:497–513
2. Karhunen PJ (1986) Benign hepatic tumours and tumour-like conditions in men. J Clin Pathol 39:183–188
3. Freeny PC, Marks WM (1986) Patterns of contrast enhancement of benign and malignant hepatic neoplasms during bolus dynamic and delayed CT. Radiology 160:613–618
4. Scatarige JC, Kenny JM, Fishman EK et al (1987) CT of giant cavernous hemangioma. AJR 149:83–85
5. Powers C, Ros PR (1994) Hepatic mass lesions. In: Haaga JR, Sartoris DJ, Lanzieri CF, Zerhouni EA (eds) Computer tomography and magnetic resonance imaging of the whole body, vol 2. Mosby, St. Louis
6. Nagel HD (2004) Radiation dose issues with MSCT. In: Reiser MF, Taskahashi M, Modic M, Becker CR (eds) Multislice CT, 2nd revised edn. Springer, Berlin Heidelberg New York, pp 17–26
7. Flohr T, Stierdorfer K, Bruder H, Simon J, Schaller S (2002) New technical developments in multislice CT. RoFo 174:839–845
8. Brix G, Nagel HD, Stamm G et al (2003) Radiation exposure in multi-slice versus single-slice spiral CT: results of a nationwide survey. Eur Radiol 13:1979–1991
9. Cohnen M, Poll LJ, Puettmann C, Ewen K, Saleh A, Modder U (2003) Effective doses in standard protocols for multi-slice CT scanning. Eur Radiol 13:1148–1153
10. Wedegartner U, Lorenzen M, Nagel HD et al (2004) Image quality of thin- and thick-slice MSCT reconstructions in low-contrast objects (liver lesions) with equal doses. Rofo 176:1676–1682
11. Flohr TG, Schaller S, Stierstorfer K, Bruder H, Ohnesorge BM, Schoepf UJ (2005) Multi-detector row CT systems and image-reconstruction techniques. Radiology 235:756–773
12. Kopka L, Rodenwaldt J, Hamm B (2001) Biphasic multi-slice helical CT of the liver: intraindividual comparison of different slice thicknesses for the detection and characterization of focal liver lesions. Radiology 217:367
13. Haider MA, Amitai MM, Rappaport DC et al (2002) Multi-detector row helical CT in preoperative assessment of small (< or = 1.5 cm) liver metastases: is thinner collimation better? Eur Radiol 225:137–142
14. Craig GR, Peters RL, Edmondson HA (1989) Tumors of the liver and intrahepatic bilde ducts. Atlas of tumor pathology, 2nd series. Armed Forces Institute of Pathology, Washington, DC

15. Schwartz LH, Gandras EJ, Colangelo SM, Ercolani MC, Panicek DM (1999) Prevalence and importance of small hepatic lesions found at CT in patients with cancer. Radiology 210:71–74
16. Khalil HI, Patterson SA, Panicek DM (2005) Hepatic lesions deemed too small to characterize at CT: prevalence and importance in women with breast cancer. Radiology 235:872–878
17. Robinson PJ, Arnold P, Wilson D (2003) Small "indeterminate" lesions on CT of the liver: a follow-up study of stability. Br J Radiol 76:866–874
18. Weg N, Scheer MR, Gabor MP (1998) Liver lesions: improved detection with dual-detector-array CT and routine 2.5-mm thin collimation. Radiology 209:417–426
19. Abdelmoumene A, Chevallier P, Chalaron M et al (2005) Detection of liver metastases under 2 cm: comparison of different acquisition protocols in four row multidetector-CT (MDCT). Eur Radiol 15:1881–1887
20. Kopp AF, Heuschmid M, Claussen CD (2001) Multidetector helical CT of the liver for tumor detection and characterization. Eur Rad 12:745–752
21. Foley WD, Mallisee TA, Hohenwalter MD (2000) Multiphase hepatic CT with multirow-detector CT scanners. AJR 175:679–685
22. Bae KT, Heiken JP, Brink JA (1998) Aortic and hepatic contrast medium enhancement at CT. Part I. Prediction with a computer model. Radiology 207:647–655
23. Brink JA (2003) Use of high concentration contrast media (HCCM): principles and rationale–body CT. Eur J Radiol 45 (Suppl 1)S53–S58
24. Marchiano A (2003) MDCT of primary liver malignancies. Eur Radiol 13: M26–M30
25. Heiken JP, Brink JA, McClennan BL, Sagel SS, Crowe TM, Gaines MV (1995) Dynamic incremental CT: effect of volume and concentration of contrast material and patient weight on hepatic enhancement. Radiology 195:353–357
26. Brink JA, Heiken JP, Forman HP, Sagel SS, Molina PL, Brown PC (1995) Hepatic spiral CT: reduction of dose of intravenous contrast material. Radiology 197:83–88
27. Miller DL, Simmons JT, Chang R (1987) Hepatic metastases detection: comparison of three CT contrast enhancement methods. Radiology 165:65
28. Nelson RC, Chezmar JL, Sugarbaker PH, Bernadino ME (1989) Hepatic tumors: comparison of CT during arterial portography, delayed CT, and MR imaging for preoperative evaluation. Radiology 172:27
29. Awai K, Hiraishi K, Hori S (2004) Effect of contrast material injection duration and rate on aortic peak time and peak enhancement at dynamic CT involving injection protocol with dose tailored to patient weight. Radiology 230:142–150
30. Itoh S, Ikeda M, Achiwa M, Ota T, Satake H, Ishigaki T (2003) Multiphase contrast-enhanced CT of the liver with a multislice CT scanner. Eur Radiol 13:1085–1094
31. Foley WD, Hoffmann RG, Quiroz FA, Kahn CE Jr, Perret RS (1994) Hepatic helical CT: contrast material injection protocol. Radiology 192:367–371
32. Roos JE, Desbiolles LM, Weishaupt D et al (2004) Multi-detector row CT: effect of iodine dose reduction on hepatic and vascular enhancement. Rofo 176:556–563
33. Takada K, Awai K, Onishi H et al (2001) Detectability of hepatocelluar carcinoma by dynamic scan with multidetector row helical CT after injection of different contrast material concentration. Radiology 217:168
34. Awai K, Hori S (2003) Effect of contrast injection protocol with dose tailored to patient weight and fixed injection duration on aortic and hepatic enhancement at multidetector-row helical CT. Eur Radiol 13:2155–2160
35. Yagyu Y, Awai K, Inoue M et al (2005) MDCT of hypervascular hepatocellular carcinomas: a prospective study using contrast materials with different iodine concentrations. AJR 184:1535–1540
36. Awai K, Takada K, Onishi H, Hori S (2002) Aortic and hepatic enhancement and tumor-to-liver contrast: analysis of the effect of different concentrations of contrast material at multi-detector row helical CT. Radiology 224:757–763
37. Awai K, Inoue M, Yagyu Y et al (2004) Moderate versus high concentration of contrast material for aortic and hepatic enhancement and tumor-to-liver contrast at multi-detector row CT. Radiology 233:682–688
38. Hirano T, Ogura K, Kumagai A et al (2003) Contrast injection protocols using dual head injector. Jpn J Radiol Technol 59:247–248
39. Tatsugami F, Matsuki M, Kani H, Miyao M, Yoshikawa S, Narabayashi I (2003) Effect of contrast material pushed with saline solution using dual injection on enhancement of aorta, portal vein, and liver parenchyma in multislice CT of the liver. Nippon Igaku Hoshasen Gakkai Zasshi 63:409–411
40. Dorio PJ, Lee FT Jr, Henseler KP et al (2003) Using a saline chaser to decrease contrast media in abdominal CT. Eur Radiol 180:929–934
41. Sandstede JJ, Tschammler A, Beer M, Vogelsang C, Wittenberg G, Hahn D (2001) Optimization of automatic bolus tracking for timing of the arterial phase of helical liver CT. Eur Radiol 11:1396–1400
42. Itoh S, Ikeda M, Achiwa M, Satake H, Iwano S, Ishigaki T (2004) Late-arterial and portal-venous phase imaging of the liver with a multislice CT scanner in patients without circulatory disturbances: automatic bolus tracking or empirical scan delay? AJR 14(9): 1665–1673
43. Van Hoe L, Marchal G, Baert AL, Gryspeerdt S, Mertens L (1995) Determination of scan delay time in spiral CT-angiography: utility of a test bolus injection. J Comput Assist Tomogr 19:216–220
44. Zandrino F, Curone P, Benzi L, Musante F (2003) Value of an early arteriographic acquisition for evaluating the splanchnic vessels as an adjunct to biphasic CT using a multislice scanner. Eur Radiol 13:1072–1079
45. Tanikake M, Shimizu T, Narabayashi I et al (2003) Three-dimensional CT angiography of the hepatic artery: use of multi-detector row helical CT and a contrast agent. Eur Radiol 227:883–889
46. Oliver JH III, Baron RL, Federle MP et al (1997) Hypervascular liver metastases: do unenhanced and hepatic arterial phase CT images affect tumor detection? Radiology 205:709–715
47. Takaki H, Yamakado K, Nakatsuka A et al (2000) Lesion detectability of hypervascular hepatocellular carcinoma with dynamic enhanced dual-arterial phase multidetector-row CT. Radiology 217:367
48. Murakami T, Kim T, Takamura M et al (2001) Hypervascular hepatocellular carcinoma: detection with double arterial phase multi-detector row helical CT. Radiology 218:763–767
49. Francis IR, Cohan RH, McNulty NJ et al (2003) Multidetector CT of the liver and hepatic neoplasms: effect of multiphasic imaging on tumor conspicuity and vascular enhancement. AJR 180:1217–1224
50. Winston CB, Koea J, Teitcher JB et al (2001) 3D CT angiography of the liver performed on a multidetector CT scanner. Radiology 217:417

51. Soyer P, Poccard M, Boudiaf M et al (2004) Detection of hypovascular hepatic metastases at triple-phase helical CT: sensitivity of phases and comparison with surgical and histopathologic findings. AJR 231:413–420
52. Valette PF, Pilleul F, Crombé-Ternamian A (2003) MDCT of benign liver tumors and metastases. Eur Radiol 13:M31–M41
53. Ishak KG (1975) Benign tumors of the liver. Med Clin North Am 59:995
54. Freeny PC, Grossholz M, Kaakaji K, Schmiedl UP (2003) Significance of hyperattenuating and contrast-enhancing hepatic nodules detected in the cirrhotic liver during arterial phase helical CT in pre-liver transplant patients: radiologic-histopathologic correlation of explanted livers. Abdom Imaging 28:333–346
55. Dähnert W (1993) Liver, bile ducts, pancreas, and spleen. In: Radiology review manual. Williams & Wilkins, Baltimore
56. Glazer GM, Aisen AM, Francis IR, Gyves JW, Lande I, Adler DD (1985) Hepatic cavernous hemangioma: magnetic resonance imaging. Radiology 155:417
57. Itai Y, Ohtomo K, Furui S (1985) Noninvasive diagnosis of small cavernous hemangioma of the liver: advantage of MRI. AJR 145:1195
58. Ros PR, Menu Y, Vilgrain V, Mortele KJ, Terris B (2001) Liver neoplasms and tumor-like conditions. Eur Radiol 11:S145–S165
59. Ros (2000) Benign liver tumors. Eur Radiol 10(S2):175–184
60. Vilgrain V, Boulos L, Vullierme MP, Denys A, Terris B, Menu Y (2000) Imaging of atypical hemangiomas of the liver with pathologic correlation. Radiographics 20:379–397
61. Gaa J, Saini S (1990) Hepatic cavernous hemangioma: diagnosis by means of rapid dynamic nonincremental CT. In: Ferrucci HT, Stark DD (eds) Liver imaging. Andover Med, Boston, pp 212-216
62. Langer R, Langer M, Felix R et al (1990) Hepatic cavernous hemangioma. A comparison of diagnostic technics. Rontgenpraxis 43:65–73
63. Choi BI, Han MC, Park JH, Kim SH, Han MH, Kim CW (1989) Giant cavernous hemangioma of the liver: CT and MR imaging in 10 cases. AJR 152:1221
64. Hanafusa K, Ohashi I, Himeno Y, Suzuki S, Shibuya H (1995) Hepatic hemangioma: findings with two-phase CT. Radiology 196:465–469
65. Byun JH, Kim TK, Lee CW et al (2004) Arterioportal shunt: prevalence in small hemangiomas versus that in hepatocellular carcinomas 3 cm or smaller at two-phase helical CT. AJR 232: 354–360
66. Cronan JJ, Esparza AR, Dorfman GS, Ridlen MS, Paolella LP (1988) Cavernous hemangioma of the liver: role of percutaneous biopsy. Radiology 166:135–138
67. Kim T, Federle MP, Baron RL, Peterson MS, Kawamori Y (2001) Discrimination of small hepatic hemangiomas from hypervascular malignant tumors smaller than 3 cm with three-phase helical CT. Radiology 219:699–706
68. Fechner RE (1977) Benign hepatic lesions and orally administered contraceptives. A report of seven cases and a critical analysis of the literature. Hum Pathol 8:255
69. Felix R, Langer R, Langer M (eds) Benign primary liver tumors. In: Diagnostic imaging in liver disease. Springer, Berlin, pp 106
70. Mathieu D, Zafrani ES, Anglade MC, Dhumeaux D (1989) Association of focal nodular hyperplasia and hepatic hemangioma. Gastroenterology 97:154
71. Welch TJ, Sheedy PF, Johnson CM (1985) Focal nodular hyperplasia and hepatic adenoma: comparison on angiography, CT, US, and scintigraphy. Radiology 156:593
72. Mathieu D, Vilgrain V, Mahfouz A-E et al (1997) Benign liver tumors. MRI Clin North Am 5:255–258
73. Dachman AH, Ros PR, Goodman ZD et al (1987) Nodular regenerative hyperplasia of the liver: clinical and radiologic observations. AJR 148: 717–722
74. Grazioli L, Morana G, Kirchin MA, Schneider G (2005) Accurate differentiation of focal nodular hyperplasia from hepatic adenoma at gadobenate dimeglumine-enhanced MR imaging: prospective study. Radiology 236(1): 166–177
75. Fabre M, Neyra M (1995) Role of fine-needle puncture in the diagnosis of a hepatic mass. Ann Pathol 15:380–387
76. Ros PR (1990) Computed tomography-pathologic correlations in hepatic tumors. In: Ferrucci JT, Matheiu DG (eds) Advances in hepatobiliary radiology. Mosby, St Louis, pp 75–108
77. Ruppert-Kohlmayr AJ, Uggowitzer MM, Kugler C, Zebedin D, Schaffler G, Ruppert GS (2001) Focal nodular hyperplasia and hepatocellular adenoma of the liver: differentiation with multiphasic helical CT. AJR 176: 1493–1498
78. Klein D, Jenett M, Gassel HJ, Sandstede J, Hahn D (2004) Quantitative dynamic contrast-enhanced sonography of hepatic tumors. Eur Radiol 14:1082–1091
79. Bartolotta TV, Midiri M, Quaia E et al (2005) Benign focal liver lesions: spectrum of findings on SonoVue-enhanced pulse-inversion ultrasonography. Eur Radiol 15:1643–1649